Available online at www.sciencedirect.com

ScienceDirect

journal homepage: www.elsevier.com/locate/jtte

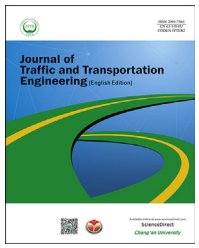

Original Research Paper

Curved footbridges supported by a shell obtained through thrust network analysis

Luigi Fenu [a,*], *Eleonora Congiu* [a], *Davide Lavorato* [b], *Bruno Briseghella* [c], *Giuseppe Carlo Marano* [c,d]

[a] *Department of Civil and Environmental Engineering, and Architecture, University of Cagliari, Cagliari 09124, Italy*
[b] *Department of Architecture, University of Roma Tre, Roma 00154, Italy*
[c] *College of Civil Engineering, Fuzhou University, Fuzhou 350116, China*
[d] *Department of Sciences of Civil Engineering and Architecture, Polytechnic University of Bari, Bari 70126, Italy*

HIGHLIGHTS

- An anticlastic shell supporting a footbridge curved deck was shaped using thrust network analysis (TNA) in non-standard way.
- The medium surface of the footbridge shell was obtained via a network nodes interpolation.
- A torsional moment induced by prestressing the ring box girder limited the transverse deflections in the cantilevered deck.
- The structural behaviour of the shell supported footbridge was confirmed by the results of the finite element (FE) analysis.

ARTICLE INFO

Article history:
Received 20 June 2018
Received in revised form
19 October 2018
Accepted 24 October 2018
Available online 18 December 2018

Keywords:
Shell footbridges
Cantilevered deck
Anticlastic shell
Thrust network analysis (TNA)
Concrete

ABSTRACT

After Maillart's concrete curved arch bridges were built before the Second World War, in the second half of the past century and this century, many curved bridges have been built with both steel and concrete. Conversely, since the construction of Musmeci's shell supported bridge in Potenza, few shell bridges have been constructed. This paper explains how to design a curved footbridge supported by an anticlastic shell by shaping the shell via a thrust network analysis (TNA). By taking advantage of the peculiar properties of anticlastic membranes, the unconventional method of shaping a shell by a TNA is illustrated. The shell top edge that supports the deck has an assigned layout, which is provided by the road curved layout. The form of the bottom edge is obtained by the form-finding procedure as a thrust line, by applying the thrust network analysis (TNA) in a non-standard manner, shaping the shell by applying the boundary conditions and allowing relaxation. The influence of the boundary conditions on the bridge shape obtained as an envelope of thrust lines is investigated. A finite element analysis was performed. The results indicate that the obtained shell form is effective in transferring deck loads to foundations via compressive stresses and taking advantage of concrete mechanical properties.

* *Corresponding author*. Tel.: +39 070 675 5434.
E-mail address: lfenu@unica.it (L. Fenu).

Peer review under responsibility of Periodical Offices of Chang'an University.
https://doi.org/10.1016/j.jtte.2018.10.007

1. Introduction

The optimal shape of shell supported bridges, especially curved bridges, is an attractive challenge for engineers. If the shell is constructed with concrete, the tensile stresses must be minimised and limited by the low tensile strength of concrete, whereas the compressive stresses must be prevalent throughout the shell and lower than the allowable compressive stress, which is generally significantly higher than the allowable tensile stress (Fenu and Madama, 2004; Flügge, 1960; Musmeci, 1971).

Therefore, the design objective is to obtain a shell that is compressed in any direction. The form-finding is performed using structural optimization algorithms (Fenu et al., 2018; Lan et al., 2017; Trentadue et al., 2018; Zordan et al., 2014), which must be robust and efficient due to the high number of discrete variables. Evolutionary algorithms are generally employed (Marano et al., 2014; Quaranta et al., 2014).

For shaping anticlastic shells, the most important design methods are listed as follows: force density method (FDM), dynamic relaxation (DR) method, particle spring (PS) method, and thrust network analysis (TNA) (Adriaenssens et al., 2014). The particle spring (PS) method and dynamic relaxation (DR) method are the only methods that consider some elastic properties of the material but disregard the inelastic and viscous properties (Fiore et al., 2012).

In the previously mentioned methods, shell form-finding is performed by an auxiliary net structure that consists of cables when in tension or bars or in compression (similar to the TNA method). The nodes of the auxiliary net structure enable the shell surface to be obtained by interpolation.

By defining the force density as the ratio of the force in a bar over its stressed length and given the position of the fixed points, the force density method obtains the shell form by solving an equation system, without any iteration (Schek, 1974). After linearization, the system of the static equilibrium equations of the nodes (subject to external loads) of a discrete network (a shell grid that consists of compression bars or a cable net of tension cables) are solved.

Conversely, the dynamic relaxation (DR) method consists of an iterative form-finding procedure that traces the motion of each node of a discrete network subject to external loads, for small time increments (Δt), until all nodes (and therefore, the entire structure) achieve a static equilibrium state (for which their kinetic energy tends to zero), assuming their final positions and defining the optimised shape of the network structure (Day, 1965). The particle spring (PS) method discretises surfaces into networks that consist of nodes (particles with lumped masses) and bars (assumed as linear elastic springs) that connect the particles, whose stiffness approximately corresponds to the stiffness of the shell strip across the spring.

Each node that is subject to external loads, which is characterised by a number of freedom degrees between zero and three that correspond to the number of orthogonal reaction forces, can be fixed or free to move. The external forces applied to each node and the internal forces that act on the springs that connect the particles must be in equilibrium. The equilibrium of each node and the shell form are iteratively obtained (Kilian and Ochsendorf, 2006).

In this paper, the thrust network analysis (TNA) form-finding method has been applied to shape the shell that supports the deck of a curved footbridge (Fenu et al., 2015, 2016a, 2016b). The TNA method is the three-dimensional version of thrust line analysis.

Although the latter applies to two-dimensional structures such as arches and barrel vaults, the former searches for the shape of a vault that is compressed in all directions and subjected to external vertical loads. An auxiliary three-dimensional network of funicular curves is shaped (Block, 2009; Rippmann et al., 2012).

Therefore, a shell with an anticlastic surface has been chosen to support a cantilevered steel deck with a curved layout, which consists of cantilever I-beams connected to a steel ring box girder.

An external prestressing system applied to the top flange of the ring box girder enabled a considerable reduction in the transverse deflections of the cantilever deck (spans 4 m from the girder). To reduce transverse deflections at the service limit state, an internal torsional moment that counteracts the external moment produced by the cantilever I-beams of the deck is induced in the box girder by prestressing it. External and internal pretensioning systems are used not only in concrete structures, but also in steel and even in stone structures (Briseghella et al., 2010a,b; Huang et al., 2012; Milan et Simonelli, 2001). Since the top edge of the concrete shell has to continuously support the cantilevered deck at its inner edge, it must have the same curvature of the given deck layout. Since the shell surface must be anticlastic, the curvature of the shell top edge and the shell meridians along the top edge must have the opposite sign. These boundary conditions and the conditions assigned to the abutments along the ground slope determine the shell shape obtained via the TNA method.

2. Historical background

2.1. *Curved bridges*

Maillart's Schwandbach Bridge (Fig. 1(a)) near Hinterfultigen, which dated to 1933, was the first curved arch bridge constructed with concrete (Bill and Maillart, 1955).

After the construction of Mallart's concrete curved bridges, few curved bridges were built until the 1980s. In these years, a great impetus to their construction was Jörg Schlaich's work. His curved bridges were the outcome of his studies on their conceptual design, which is described by some simple but very significant structural schemes on their working principles, as described in Schlaich and Bergermann (2004) and illustrated by a large-scale steel model in the Science and Technology Museum in Munich.

In particular, his studies on prestressing the deck of curved bridges to favourably exploit its curved layout by torsional moments, which counteracts the moments induced by the applied loads, are a milestone in the history of curved bridges.

After his first curved suspended bridge in Kelheim, over the canal between the Rheine and Danube (Schlaich and Bergermann, 2004), with a curved deck girder that is constructed with prestressed concrete, where stresses

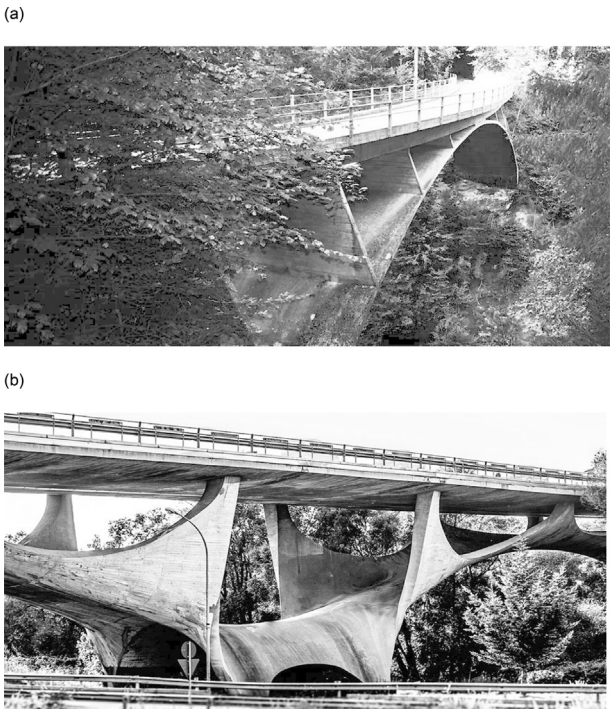

Fig. 1 – Curved bridges. (a) Maillart's Schwandbach Bridge, Switzerland. (b) Musmeci's shell bridge over the Basento River in Potenza, Italy.

flowed in the "black box" of the concrete deck. Schlaich et al. (1987) designed several suspended and cable-stayed curved footbridges with internal forces that flow into structural elements that are specifically designed to bear them.

A comparison of the static functioning of the decks of two of Schlaich's beautiful curved suspended footbridges—the Bochum Bridge and the Reedy River Bridge—are suspended at the inner edge and the outer edge, respectively, is noteworthy (Schlaich et al., 1987). In the Bochum Bridge (Fig. 2(a)), the axial force in the lower chord of the curved girder (with curvature radius *R*) and the horizontal projection of the axial force in the hanger can provide a sufficiently high counter-moment (with lever arm *Z*) to the external lifted load (with lever arm *e* to the hanger restraint). A prestressing system was applied to the top flange of the ring girder. Prestressing the deck girder at its top would have provided an increased counter-moment that would have been necessary only if higher external loads had been applied.

Due to the deck layout and the landscape view, the deck of the curved suspended bridge over the Reddy River in Greenville, S.C., USA (Fig. 2(b)), is suspended at its outer edge, which reverses the direction of the deck curvature radius *R* with respect to the Bochum Bridge.

The suspension of the deck at the outer edge causes the inversion of the direction of the flow of the internal forces with respect to the Bochum Bridge (suspended at its inner edge). In the Reedy River Bridge, the tensile forces provided by three ring tension cables positioned at the girder bottom, refer to Fig. 2(b) flow at the intrados of the ring girder, whereas compressions flow in the upper concrete deck. Pretensioning the ring girder reduces the transverse deflections of the cantilever deck by counteracting the moment produced by the external load lifted (with lever arm *e* to the hanger restraint) by inducing a moment that acts in the transverse direction (with lever arm *Z*).

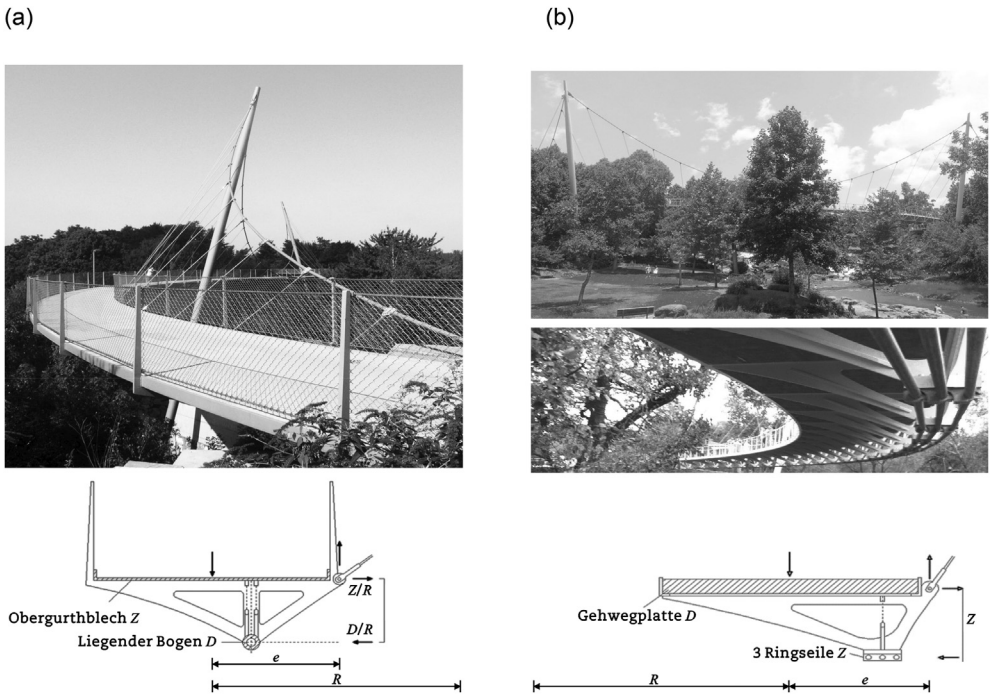

Fig. 2 – Schlaich's suspended curved footbridges with details of their deck cross-sections. (a) Bochum Bridge, Germany. (b) Reedy River Bridge, USA.

2.2. *Shell-supported bridges*

Concrete shell structures have been studied by masters in structural architecture, such as Frei Otto (Otto et al., 1973), Heinz Isler (Isler, 1994) and Sergio Musmeci (Musmeci, 1971). They modelled their compressed shells by auxiliary tension structures with the same shape but with internal forces and constraint reactions of the opposite sign for the same boundary conditions and self-weight loading.

If the auxiliary tension structures were constructed with isotropic materials, a shell of minimal surface was obtained. Conversely, when an anisotropic auxiliary tension structure with anisotropic curvatures was to be obtained (such as the Basento shell supported bridge with transverse curvatures that are significantly higher than longitudinal curvatures), Musmeci constructed physical models using materials capable of developing anisotropic stresses (such as neoprene).

A shell-supported road bridge designed by Alfred Pauser was constructed in Eldberger, Austria, from 1968 to 1971. In the same period, Musmeci constructed the first concrete bridge supported by an anticlastic concrete shell—the Basento Bridge in Potenza, Italy (Fig. 1(b))—Musmeci's masterpiece designed in the 1960s and built between 1967 and 1976 (Musmeci, 1971). In the first years of this century, Jiri Strasky proposed two shell-supported footbridges in two international design competitions: the first competition was held in Jersey (UK), and the second competition was held in London for the Leamouth Footbridge (Strasky, 2007). In Madrid, Hugo Corres Peiretti designed the Matadero Bridge in 2011, which was a pedestrian bridge whose deck is suspended to a sinclastic shell (a concrete canopy that covers the bridge) by several hangers (Balázs et al., 2016; Corres-Peiretti et al., 2012).

A comparison of the differences between the structural functioning of Maillart's bridges (Bill and Maillart, 1955) and the structural functioning of Musmeci's bridge (Nicoletti and Musmeci, 1999) is noteworthy.

For the first time in the history of arch bridge construction, Maillart's bridges were the first stone (artificial) arch bridges with no infill over the arch. Musmeci substituted vertical walls and arch through a continuous anticlastic shell of minimal surface to continuously transfer the deck loads from the shell restraints that support the deck to the shell foundations, which prevented undesired bending effects due to the insertion of vertical walls in the shell arch, similar to Maillart's bridges.

Fenu et al. (2006) compared the structural behaviour of a bridge with a deck supported by an anticlastic shell that is compressed in any direction with a Maillart's bridge with the same span and rise (the Traubach Bridge near Habkern described in Bill and Maillart (1955).

Briseghella et al. applied topology optimization to arch bridges to reduce the bridge self-weight and the seismic action on the foundations and applied topology optimization to shell supported bridges to reduce the area of the shell regions, where unwished tensile stresses can arise (Briseghella et al., 2013a, 2013b, 2016; Zordan et al., 2010). Fenu et al. applied the particle spring method for the form-finding of a concrete anticlastic shell that supports the curved deck of a shell-supported footbridge, as illustrated in (Fenu et al., 2015).

3. Thrust network analysis (TNA) form-finding procedure

A thrust network is a three-dimensional version of the thrust curve of a unidimensional structure that lies in a plane. Using techniques derived from "graphic statics", TNA extends the "thrust line analysis" to spatial networks for the specific case of external loads that are only applied in the vertical direction. Therefore, a thrust network analysis is a form-finding method for designing shell structures compressed in any direction as an envelope of thrust lines (Adriaenssens et al., 2014). The method is independent of material properties. It was developed (and is particularly suitable) for designing masonry vaults that should be compressed in any direction due to the low tensile strength of masonry.

The TNA method is based on the assumption (derived from descriptive geometry) that a three-dimensional network under vertical external loads is in compression when its projection on the horizontal plane is also in compression.

The form-finding of the optimal shell shape by a thrust network analysis method is performed by the simultaneous manipulation of two diagrams: the form diagram Γ, which is the horizontal projection of the three-dimensional network G, and the force diagram Γ^*, which is constituted by the horizontal components of the forces that act on each bar of the compressed network.

Form and force diagrams are dual graphs that are reciprocally related to each node of Γ that corresponds to an equilibrium polygon of Γ^*. The side number of the force polygon in equilibrium at this node is equal to the number of branches that join in the corresponding node of Γ, and vice versa. Each side of all polygons of Γ and the corresponding force of the related equilibrium polygon in Γ^* must be parallel (within a certain tolerance angle that is generally included between 5° and 10°). From a structural point of view, the equilibrium of a node in one graph is guaranteed by a closed polygon of force vectors in the other graph, and vice versa. The length of each branch e^* of the force diagram Γ^*, multiplied by an assigned scale factor ς, provides the magnitude of the axial force that acts in the corresponding branch e of the form diagram Γ, and the magnitude of the horizontal component of the axial force that acts on the corresponding bar of the three-dimensional thrust network G (Schek, 1974).

The geometric reciprocal relationships between Γ and Γ^* are true regardless of the size of Γ^*.

The reciprocal relationship between Γ and Γ^* cannot (by themselves) guarantee that all network bars are in compression. This additional condition is satisfied only if the vectors of all closed polygons of Γ rotate counterclockwise with respect to any point inside the closed polygon.

All polygons of Γ and Γ^* must be convex to prevent the formation of tension forces or tensile stresses in any shell regions, as required when the tensile strength is negligible as in the concrete shell under consideration.

In its original formulation, TNA generates a funicular network of bars, where only external loads in the vertical direction are considered. Therefore, the equilibrium of the horizontal force components is to be considered; it can be

computed independently of the external vertical loading. In the 3D thrust network that is subsequently obtained, the equilibrium with any vertical force is satisfied (Adriaenssens et al., 2014), provided that the effective constraint is defined.

The form-finding process can be divided into two distinct phases:

- solving horizontal equilibrium;
- solving vertical equilibrium.

The equilibrium polygon of the force diagram can be statically indeterminate. While the three forces in equilibrium in a closed force diagram bi-univocally correspond to the three branches that meet at a node of the form diagram and are parallel to the corresponding forces, the network is statically indeterminate when more than three vectors meet in each node of Γ, even if the parallelism condition is satisfied. For a given form diagram Γ, many force diagrams can exist, which enables the redistribution of the internal forces in the structure. In this case, among all feasible force diagrams Γ^*, the designer chooses the diagram where, for instance, compressions are smaller than an allowable given value.

For a chosen horizontal equilibrium solution, multiple vertical equilibrium solutions that correspond to different shell shapes can be obtained by the TNA method, depending on the allowed redistribution of the internal forces, which causes network relaxation. By allowing relaxation, the horizontal components of the forces of the 3D thrust network are reduced. Conversely, lower relaxation indicates an increase in the horizontal components of the thrust network forces.

The lower the network relaxation, the higher the internal forces in the thrust lines and the compression stresses in the shell, as verified by a finite element analysis (FEA) to verify whether the compression stresses are lower than the concrete allowable compression stress. Therefore, if the stresses are too high, we can allow relaxation and achieve a new shell shape; if the stresses are too low, less relaxation could be allowed.

Note that the boundary conditions must be suitably assigned for TNA to shape an anticlastic shell.

The larger the increase in the stresses in one direction, the larger the increase in the other directions, which is easily checked by the FEA. The stress level can also be modified by the shell thickness, which indicates that the stresses are reduced by the larger cross-sectional area if the shell thickness is changed; however, dead loads are also changed, which can be considered by the FEA.

Using the described graphic procedure, the thrust network analysis obtains the optimum shape for compressed networks of any typology. The procedure can also be analytically implemented, as exhaustively illustrated in Adriaenssens et al. (2014).

3.1. *Applying TNA to find the form of the shell that supports a curved bridge deck*

In this section, the design problem of shaping a concrete shell, which is compressed in any direction and supports the curved deck of a footbridge, is addressed.

By providing appropriate boundary conditions, the form-finding procedure solves the design problem by shaping an anticlastic shell, which minimises undesired tensile stresses.

Contrary to straight shell-supported bridges, where deck stability is guaranteed if the deck is supported by the shell along two parallel lines (similar to the deck of Musmeci's Bridge, refer to Fig. 1(b)), a curved deck can be supported along one curved line, as allowed by the static equilibrium conditions of simply supported ring girders. This design solution is adopted in Schlaich's curved bridges and illustrated in Section 2.1. This solution has also been adopted in the curved shell bridge that is considered in this study.

As the curved layout of the deck depends on the given curved layout of the pedestrian route, a first boundary condition is that the curvature of the parallel of the shell along its top edge must coincide with the deck curvature. As the shell must be anticlastic (otherwise, tensile stresses cannot be minimised), the meridian curvatures along the shell top edge must have the opposite sign with respect to the curvature of the deck.

In addition to these boundary conditions that are governed by the given layout of the deck, additional boundary conditions for the shell must be defined at the bridge abutments along the ground slope (Fig. 3(a)). By suitably defining these boundary conditions, the differences between the opposite curvatures in each point of the anticlastic surface can be increased, which optimises the shell form to minimise the tensile stresses throughout the shell. Topology optimization of the shell restraint position at the abutments was performed.

The form-finding of a shell using TNA typically begins on a flat surface, which has to represent the potential shell projection on the horizontal plane. However, when using TNA to find the form of a shell supporting the deck of a curved footbridge (Fenu et al., 2016a,b), the TNA (at least in the original version proposed by Block (2009)) must consider that it can only govern the form finding of a shell whose projection on the horizontal plane cannot be overlapped by the projection of any other shell region. Unfortunately, the shell of the footbridge under consideration does not satisfy this condition. Solving the form-finding problem for different boundary conditions with physical models revealed that an anticlastic shell can be obtained only if this condition was not satisfied.

By projecting the shell surface in the vertical plane orthogonal to the deck curvature radius at mid-span, the vertical projection of any shell region can biunivocally correspond to the shell surface without overlapping any vertical projection of other shell regions.

Therefore, the TNA method was applied in a non-standard manner by drawing form and force diagrams in this vertical plane, shaping the shell by applying the boundary conditions and allowing relaxation in the horizontal direction, as the shell was subjected to horizontal forces without gravity.

A stepwise procedure was adopted. A starting surface reasonably close to the potential vertical projection of the shell surface (Fig. 3(b)) was initially considered. After at least one attempt, the initial surface was modified to be closer to the vertical projection of the shell that would have been

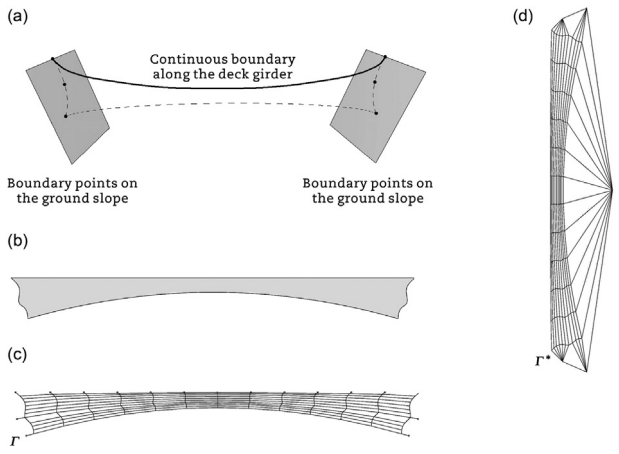

Fig. 3 – Initial conditions and diagrams of the thrust network analysis. (a) Boundary conditions. (b) Starting surface. (c) Initial form Γ. (d) Force Γ^* diagrams.

obtained by the form-finding procedure. The larger the number of attempts, the closer the starting surface to the final vertical projection of the shell obtained by the form-finding procedure.

Initial form and force diagrams were constructed in the vertical plane orthogonal to the curvature radius of the deck at mid-span. In the initial form diagram, the first tentative directions of the internal forces that act throughout the shell are attempted to obtain the initial force diagram until an initial form diagram Γ and an initial force diagram Γ^* (Fig. 3(d)) that satisfies the reciprocity condition between them is drawn.

As the form diagram Γ was subdivided into four-sided polygons, the equilibrium of each node of Γ in the projection plane is represented by closed quadrilateral convex force polygons. In this case, one degree of indeterminacy and the obtained force diagram represents one of the infinite possible equilibrium states for G in the projection plane.

Note that the branches of the force diagram correspond to the forces that act along the free edges of the spatial network G assuming a peculiar fan configuration that represents the equilibrium polygons of the nodes along the free edges of the thrust network.

Step by step, form and force diagrams converged to equilibrium in the vertical projection plane until the reciprocity condition and the parallelism condition that was defined in the previous section were satisfied. The final diagrams Γ (Fig. 4(a)) and Γ^* (Fig. 4(b)) were achieved. In addition to the form diagram equilibrium, the equilibrium of network G was satisfied, regardless of the loads that are orthogonal to the projection plane. For the sake of precision, only solutions with less than one degree of deviation from the parallelism condition were accepted.

Fig. 4(c) shows the boundary points in the 3D space, which are obtained by defining the distances of the support fixed nodes z_F from the projection plane. By stretching the branches of the planar form diagram Γ to satisfy the boundary conditions not only in the projection plane but also in the 3D space for the third coordinate z_F of the fixed nodes, the form of the three-dimensional thrust network was obtained (Fig. 4(d)), and the distances of the unsupported nodes z_N from the projection plane were established.

The shell shaping was performed by contemporarily checking if the Gaussian curvature (i.e., the product of the two principal curvatures) was negative, which indicates that the shell surface was anticlastic. If the Gaussian curvatures were positive, then the boundary conditions at the abutments had to be changed to obtain negative Gaussian curvatures (as negative as possible). Different relaxation levels were allowed, and the stresses throughout the shell that were subject to real loads were checked by a finite element analysis (FEA). As illustrated in the previous section, higher relaxation corresponds to lower internal forces in the 3D network and lower compression stresses in the shell. Lower relaxation is

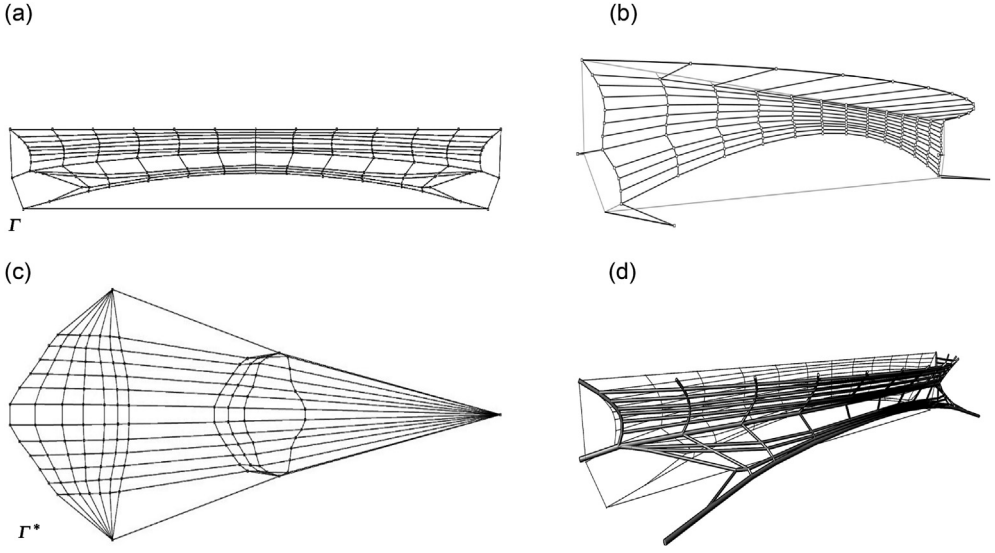

Fig. 4 – Final diagrams of the thrust network analysis. (a) Final form Γ. (b) Force Γ^*. (c) Diagrams, 3D boundary conditions. (d) Obtained network G.

associated with higher internal forces and higher compression stresses.

After trying different relaxation levels at each step, if Gaussian curvatures were acceptable and compressive stresses were higher than the allowable compressive stress, the shell thickness was increased until the maximum compressive stress was lower than the allowable stress. Conversely, if the stress level was too low even after allowing high relaxation levels, then the compressive stresses were increased by decreasing the shell thickness. Note that tensile stresses tend to increase in the compressed shell due to second-order effects and can only be minimised by the form-finding procedure by applying appropriate boundary conditions.

4. Arrangement of the curved deck

The shell was constructed with concrete with grade C 35/42. The curvature and radius (in the horizontal direction) of the shell top edge (coincides with the curvature and radius of the deck layout) were 0.0035 m^{-1} and 28.3 m, respectively. The lengths of the curved deck and the related circle chord were 44.48 and 40 m, respectively.

The cantilever deck was supported by a ring box girder with three webs (depth 550 mm, breadth 500 mm, thickness of flange and webs 20 mm, and steel grade S355) that were installed on the shell top edge. One-line steel studs spaced 500 mm connected the shell top edge to the bottom flange of the girder, which was stiffened by the inner web and transverse plates that were welded inside the box girder and positioned in correspondence of the studs.

The ring box girder consisted of 16 straight segments. The length of each segment was 2.78 m; they were connected by butt-welded joints. The cantilevered deck was constructed with cantilever I-beams spaced 2.78 m; the depth of the deck varied between 0.55 m (at the end connected to the ring girder) and 0.32 m (at the end along the deck outer edge). The cantilever I-beams supported a concrete slab, with a thickness of 0.20 m, cast on a profiled steel sheet connected to their top flange.

An external pretensioning system applied an eccentric prestress force at the top flange of the ring girder.

Three parallel tension cables (f_{ptk} = 1860 MPa, centroid distant 117.5 mm from the girder top) anchored to anchorage heads positioned over the joint that connects the girder segments, provided an eccentric axial force to the girder (Fig. 5(a) and (b)). The cross-sectional area of each cable was 2215 mm^2.

The pretensioning cables induced a longitudinal bending moment that induced a torsional moment that counteracts the moments transmitted to the girder by the cantilevered I-beams due to the intrinsic properties of ring girders and reduced the transverse deflections of the cantilever deck (Fig. 5(a) and (c)).

Fig. 6 shows a rendered image of the curved shell-supported bridge over an artificial canyon in the Tuvixeddu archaeological park of Cagliari (Italy) to better illustrate the form and the aesthetic characteristics of the bridge in an urban natural landscape.

5. Structural behaviour of the curved shell footbridge

An accurate 3-D digital model of the curved shell pedestrian bridge was initially built in Rhino and then imported in ANSYS to perform a FEM analysis. A concrete shell, concrete slab, ring box girder and I-beams were modelled with four-node shell elements, whereas the anchorage heads of the external prestress cables were modelled with eight-node solid elements. Tension cables were modelled via link elements, and

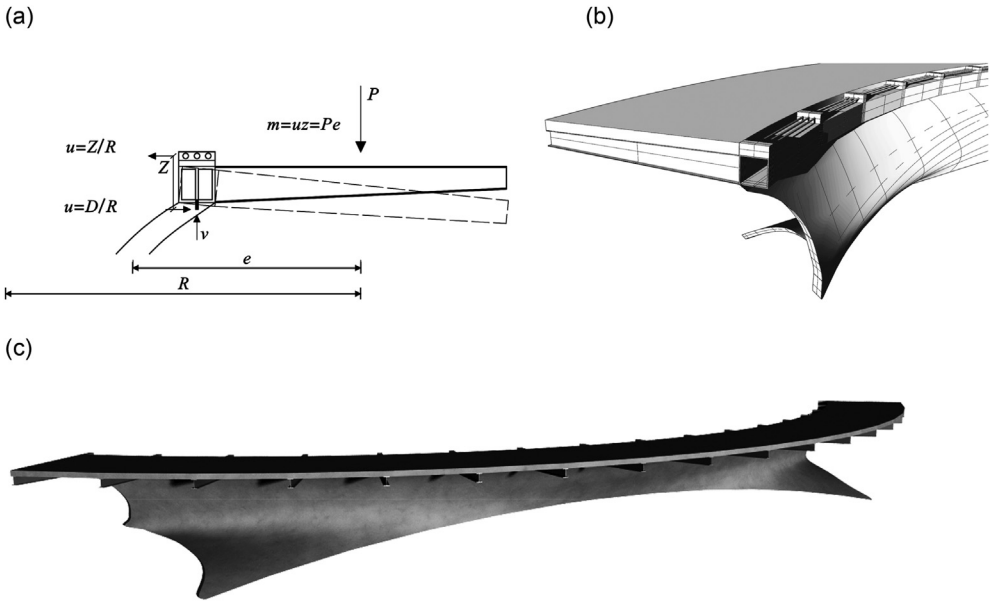

Fig. 5 – Structural scheme of the deck. (a) Transverse cross-section. (b) Detail of the three-dimensional model of the structure. (c) Three-dimensional model of the structure.

Fig. 6 – A rendered image of the curved shell-supported footbridge over an artificial canyon in the Tuvixeddu archaeological park in Cagliari, Italy.

the pre-tensioning force was induced by applying an initial deformation to the cables. The average side of the shell and solid elements was 50 mm.

In addition to the dead loads, crowd loads of 5 kN/m^2 were applied, with five load cases considered: 1) full bridge full width, 2) full bridge half width by the outer edge side, 3) full bridge half width by the inner edge side, 4) half bridge full width, 5) two diagonal areas of half width.

The shell analysis indicated that the shell was prevalently in compression with a maximum compressive stress of 18 MPa (as shown in Fig. 7(a) and (b)), which reduced the allowable strength of modern concretes. The tensile stresses minimised by the shell shape were provided by the form-finding procedure (Fig. 8(a) and (b)) and limited to 2.2 MPa in load case 3 and 2 MPa in load case 1, even if this value was attained in a small shell region throughout the shell (with the exception of the local stress concentration close to the point restraints). The first principal stress was positive (tension) but significantly lower than 1 MPa elsewhere and lower than zero (compression) throughout more than two-thirds of the shell surface.

The stress level in the steel ring box girder was higher in load case 1, especially at its ends due to the high prestress force provided by the tension cables and transmitted by the prestressing anchorage heads.

The thickness of the inner segments of the box girder was 20 mm, whereas thicker end segments were needed (40 mm) due to the high stress level close to the anchorage head of the tension cables at the girder ends. To resist this high prestress force, the steel grade S355 was adopted for the girder end segments.

Conversely, a steel grade lower than S355 was applied to the inner segments, where the stress level was lower. The force in each cable was 2500 kN (namely, a total force of 7500 kN), which corresponds to a tensile stress in the cables of 1130 MPa; the force was obtained by applying an initial strain of 0.0053.

The maximum deflection was 35.9 mm and occurred at mid-span in load case 1 (Fig. 8(c)).

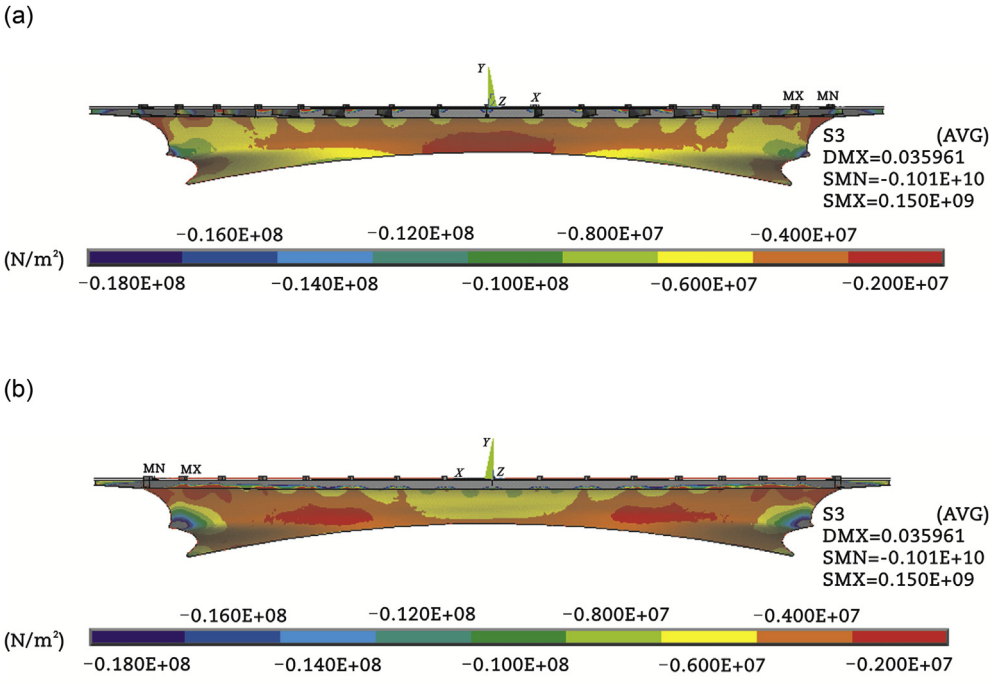

Fig. 7 – Compressive stresses throughout the shell surface. (a) Front view. (b) Back view.

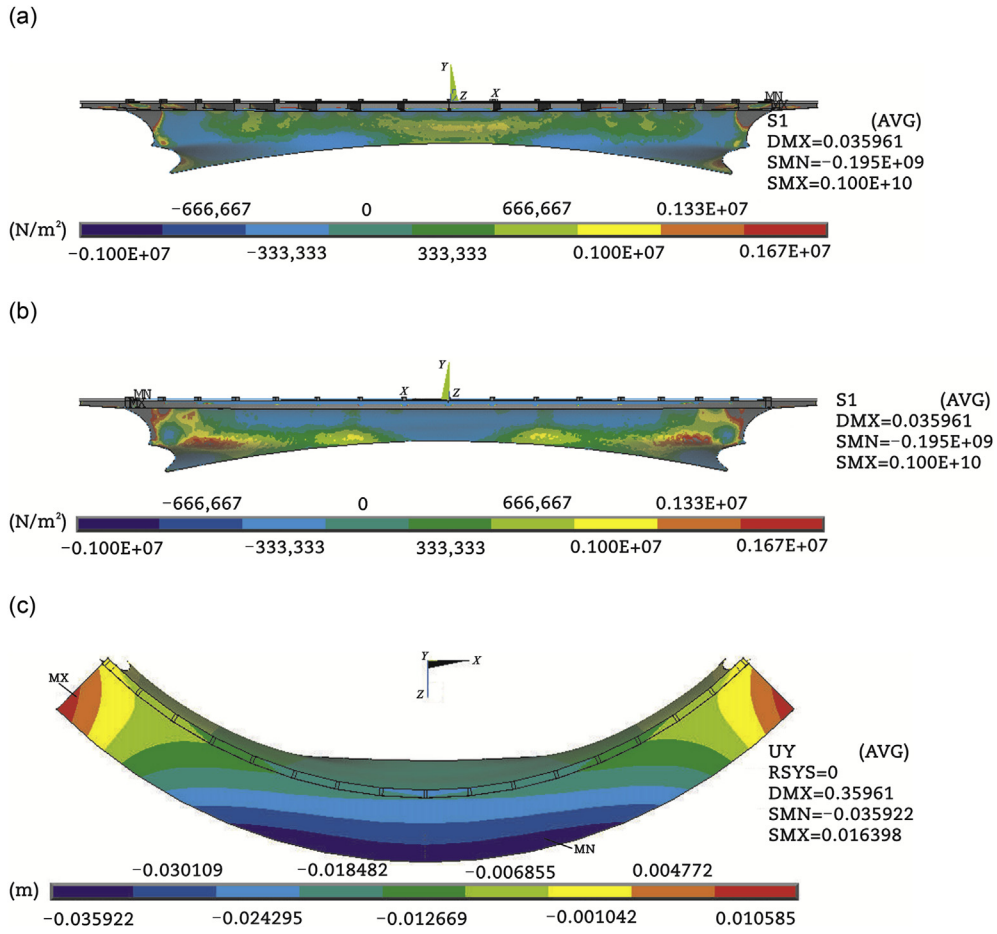

Fig. 8 – Tensile stresses throughout the shell surface. (a) Front view. (b) Back view. (c) Contour plot of the vertical displacements: top view.

The shell footbridge was very stiff, as the ratio between the span length (40,000 mm) and the maximum deflection (35.9 mm) was 1113.

The torsional counteracting moment induced by pre-stressing the ring box girder limited the transverse deflections in the cantilevered deck. In the transverse direction, the maximum deflection difference between the inner edge and outer edge of the deck was 19.3 mm. Therefore, the ratio of the double cantilever length over the deck transverse deflection was 413.

6. Conclusions

An anticlastic shell that is capable of supporting the curved deck of a footbridge was shaped using thrust network analysis in a non-standard manner, as a horizontal starting surface cannot be obtained as a shell horizontal projection without the overlapping of some shell regions. Considering the intrinsic properties of anticlastic membranes, for which compressions in one direction induce compressive stresses in any other direction, the shell was shaped by its projection in the real vertical plane that is considered in the TNA as a horizontal plane where the 2D equilibrium of the network is obtained. By taking advantage of anticlastic membrane properties, the form-finding procedure began by drawing the initial form diagram (Γ) and discretising a starting surface provided by the potential projection of the shell in the vertical plane, instead of the projection in the horizontal plane, which is generally employed in standard TNA applications. Consequently, the initial force diagram, which represents a first possible equilibrium configuration of horizontal force components, has been constructed from the initial Γ diagram (according to the reciprocity conditions described in the previous sections) on the same plane in which the form diagram lies. The original boundary conditions have been rotated 90° in the 3D space. At the end of the form-finding procedure, the forces that compose the force diagram Γ^* can be considered to be in balance with any system of vertical loads and orthogonal to the plane on which planar diagrams lie. For a chosen horizontal equilibrium configuration, TNA enables the generation of an infinite number of vertical equilibrium solutions, which are obtained by varying the relaxation level of the thrust network. As a high level of relaxation of the thrust network corresponds to lower internal forces in the network bars, and vice versa, by varying this scale factor, these forces and the stress level in the shell could be monitored. This finding explains why the unconventional manner in which the TNA method has been applied for finding an optimal shell shape

yields reasonable structural results by a FEA. After finding the 3D compressed network by this non-standard TNA application, the medium surface of the footbridge shell was obtained via a network nodes interpolation. The excellent structural behaviour of the shell supported footbridge has been confirmed by the results of the FE analysis, which demonstrated that the non-conventional form-finding procedure minimised unwished tensile stresses in the concrete anticlastic shell and that a prestressing system that is externally applied to the top flange of the ring box girder effectively reduced the maximum deflections in the loading direction.

Conflict of interest

The authors do not have any conflict of interest with other entities or researchers.

Acknowledgments

The research was supported by the Recruitment Program of Global Experts Foundation (Grant No. TM2012-27), the National Natural Science Foundation of China (Grant No. 51778148 and 51508103) and the Fujian Provincial Education Department Research Foundation for Young Teacher (Grant No. JA150743). The authors acknowledge the Sustainable and Innovative Bridge Engineering Research Center (SIBERC) of the College of Civil Engineering, Fuzhou University (Fuzhou, China) and the Department of Civil Engineering, Environmental Engineering and Architecture of University of Cagliari (Cagliari, Italy).

REFERENCES

Adriaenssens, S., Block, P., Veenendaal, D., et al., 2014. Shell Structures for Architecture. Taylor & Francis Group, New York.

Balázs, G.L., Farkas, G., Kovács, T., 2016. Reinforced and prestressed concrete bridges. In: Pipinato, A. (Ed.), Innovative Bridge Design Handbook. Elsevier Inc., Oxford, pp. 213–246.

Bill, M., Maillart, R., 1955. Girsberger. Zurich, 1955.

Block, P., 2009. Thrust Network Analysis: Exploring Three-dimensional Equilibrium (PhD thesis). Massachusetts Institute of Technology, Cambridge.

Briseghella, B., Fenu, L., Feng, Y., et al., 2013a. Topology optimization of bridges supported by a concrete shell. Structural Engineering International 23 (3), 285–294.

Briseghella, B., Fenu, L., Feng, Y., et al., 2016. Optimization indexes to identify the optimal design solution of shell-supported bridges. Journal of Bridge Engineering 21 (3), 04015067.

Briseghella, B., Fenu, L., Huang, W., et al., 2010a. Tensegrity bridge with prestressed deck. In: Large Structures and Infrastructures for Environmentally Constrained and Urbanised Areas, Zurich, 2010.

Briseghella, B., Fenu, L., Huang, W., et al., 2010b. Tensegrity footbridges with arch deck: static and dynamic behaviour. In: 6th International Conference on Arch Bridges, Fuzhou, 2010.

Briseghella, B., Fenu, L., Lan, C., et al., 2013b. Application of topological optimization to bridge design. Journal of Bridge Engineering 18 (8), 790–800.

Corres-Peiretti, H., Dieste, S., León, J., et al., 2012. New materials and construction techniques in bridge and building design. In: Fardis, M.N. (Ed.), Innovative Materials and Techniques in Concrete Construction. Springer, Dordrecht, pp. 17–41.

Day, A.S., 1965. An introduction to dynamic relaxation. Engineering 219, 218–221.

Fenu, L., Briseghella, B., Congiu, E., 2016a. Curved footbridges supported by a shell obtained as an envelope of thrust-lines. In: 8th International Conference on Arch Bridges, Wroclaw, 2016.

Fenu, L., Briseghella, B., Marano, G.C., 2018. Optimum shape and length of laterally loaded piles. Structural Engineering and Mechanics 68, 121–130.

Fenu, L., Briseghella, B., Zordan, T., 2015. Curved shell-supported footbridges. In: IABSE Conference 2015: Structural Engineering-providing Solutions to Global Challenges, Geneva, 2015.

Fenu, L., Congiu, E., Briseghella, B., 2016b. Curved deck arch bridges supported by an inclined arch. In: 19th International Association for Bridge and Structural Engineering (IABSE) Congress: Challenges in Design and Construction of and Innovative and Sustainable Built Environment, Stockholm, 2016.

Fenu, L., Madama, G., 2004. A method of shaping R/C shells with heuristic algorithms and with reference to Musmeci's work. Stud e Ric - Politec di Milano Sc di Spec Costr Cem armato 24, 199–238.

Fenu, L., Madama, G., Tattoni, S., 2006. On the conceptual design of R/C footbridges with the deck supported by shells of minimal surface. Stud e Ric - Politec di Milano Sc di Spec Costr Cem armato 26, 103–126.

Fiore, A., Monaco, P., Raffaele, D., 2012. Viscoelastic behaviour of non-homogeneous variable-section beams with post-poned restraints. Computers and Concrete 9 (5), 357–374.

Flügge, W., 1960. Stresses in Shells. Springer, Berlin.

Huang, W., Fenu, L., Briseghella, B., et al., 2012. Static behaviour of a prestressed stone arch footbridge. In: 5th International Conference on New Dimensions in Bridges, Flyovers, Overpasses and Elevated Structures, Wuyishan, 2012.

Isler, H., 1994. Concrete shells derived from experimental shapes. Structural Engineering International 4 (3), 142–147.

Kilian, A., Ochsendorf, J., 2006. Particle spring systems for structural form finding. Journal of the International Association for Shell and Spatial Structures 46 (2), 77–84.

Lan, C., Briseghella, B., Fenu, L., et al., 2017. The optimal shapes of piles in integral abutment bridges. Journal of Traffic and Transportation Engineering (English Edition) 4 (6), 576–593.

Marano, G.C., Trentadue, F., Petrone, F., 2014. Optimal arch shape solution under static vertical loads. Acta Mechanica 225 (3), 679–686.

Milan, M., Simonelli, F., 2001. Padre Pio Church, Foggia, Italy. Structural Engineering International 11 (3), 170–172.

Musmeci, S., 1971. La Statica e le Strutture. Cremonese, Roma.

Nicoletti, M., Musmeci, S., 1999. Sergio Musmeci: Organicità di Forme e Forze Nello Spazio. Testo & Immagine, Torino.

Otto, F., Trostel, R., Schleyer, F.K., 1973. Tensile Structures: Design, Structure, and Calculation of Buildings of Cables, Nets, and Membranes. The MIT Press, Cambridge.
Quaranta, G., Fiore, A., Marano, G.C., 2014. Optimum design of prestressed concrete beams using constrained differential evolution algorithm. Structural and Multidisciplinary 49 (3), 441–453.
Rippmann, M., Lachauer, L., Block, P., 2012. Interactive vault design. International Journal of Space Structures 27 (3), 219–230.
Schek, H.J., 1974. The force density method for form finding and computation of general networks. Computer Methods in Applied Mechanics and Engineering 3 (1), 115–134.
Schlaich, J., Bergermann, R., 2004. Leicht Weit/Light Structures. Prestel, Munchen.
Schlaich, J., Schafer, K., Jennewein, M., 1987. Toward a consistent design of structural concrete. Journal of the Prestressed Concrete Institute 32 (3), 74–150.
Strasky, J., 2007. Bridges utilizing high strength concrete. International Journal of Space Structures 22 (1), 61–79.
Trentadue, F., Marano, G.C., Vanzi, I., et al., 2018. Optimal arch shape for single-point-supported deck bridges. Acta Mechanica 229 (5), 2291–2297.
Zordan, T., Mazzarolo, E., Briseghella, B., et al., 2014. Optimization of Calatrava bridge in Venice. In: The 7th International Conference on Bridge Maintenance, Safety, and Management, Shanghai, 2014.
Zordan, T., Briseghella, B., Mazzarolo, E., 2010. Bridge structural optimization through step-by-step evolutionary process. Structural Engineering International 20 (1), 72–78.

Dr. Luigi Fenu graduated with master's degree in civil engineering from University of Cagliari, Italy, where he teaches structural design and is a researcher in this field. After starting his research in the field of foundation structures, now his main field of interest includes conceptual design (especially of innovative bridges) and structural optimization, together with the dynamic behaviour of materials, and the seismic behaviour of adobe buildings. He has a research fellowship at the Sustainable and Innovative Bridge Engineering Research Center (SIBERC) in the Fuzhou University (China), where he is carrying out his studies on innovative curved bridges.

Dr. Bruno Briseghella is distinguished professor and dean of the College of Civil Engineering, Fuzhou University, China, and founding director of the "Sustainable and Innovative Engineering Research Center". He graduated with a bachelor's and master's degree from Padova University, Italy, and a PhD from Trento University, Italy. His main research activities have been focused on bridge and structural design, integral abutment bridges, monitoring and retrofit of bridges, earthquake engineering and composite steel-concrete structures, both from the theoretical and experimental point of view.